Integration of Miniaturized Array Antenna With High-Permittivity Rectangular Bismuth Titanate for WiMAX Applications

Fwen Hoon Wee, F. Malek, Farid Ghani, and Azlan Umar Al-Amani

***Abstract*—High-permittivity rectangular bismuth titanate (ReBiT) array antennas for WiMAX application have been investigated, fabricated, and measured. The antennas are designed and constructed with a combination of two-, four-, and six-BiT elements in an array form stacked on a microwave substrate. The impedance bandwidth of the ReBiT is 350 MHz, and it is able to operate in the frequency range of 2.20 to 2.55 GHz, which is suitable for the application of a WiMAX 2.30 GHz system. The utilization of a bismuth titanate (BiT) ceramic that covers about 90% of the antenna led to high radiation efficiency, low cost, and the production of small-size antennas.**

***Index Terms*—Array antennas, bismuth titanate, low-loss antenna, WiMAX.**

I. Introduction

Ceramic antennas (CAs) have become attractive due to their particular advantages for some applications, including zero conductor loss and low profile [1]–[8]. Various CA approaches have been described in the literature [1]–[12]. CAs with various shapes has been designed using a microstrip patch connected through a microstrip feeder [1]. An array of 3×3 CAs was designed with a size of 60 mm $\times$ 40 mm and that operated at 5.8 GHz. Results of 60-MHz bandwidth and 10-dB gain were reported [1]. Ref [3] presented a fractal rectangular CA for WiMAX application with a permittivity $\varepsilon' = 20$. The design dimensions were $20\ \mathrm{mm} \times 12\ \mathrm{mm} \times 13\ \mathrm{mm}$, and the ground plane size was 50 mm $\times$ 50 mm. The gain and directivity were 5.998 dB and 6.009 dB, respectively. Analysis of magnetic and electric properties on a 10-cm diameter disc with an antenna high miniaturization factor of 7–10 was reported in [4]. The need for miniaturization most probably is more important for lower frequency bands at which the wavelengths are longer. However, this communication proved that high-frequency antenna designs also can achieve miniaturization but with a limited miniaturization factor due to the original small size.

Among all microwave transmission lines, the BiT ceramic feature offers extremely low losses up to a very high dielectric constant. For this reason, such devices have been utilized intensively as radiation patches and in the special feed system of planar arrays. Owing to these characteristics, the array elements will show high radiation efficiency, higher gain, and allow the production of miniaturized antennas.

In this study, we proposed a novel CA with a new branching structure that uses ceramic material. This CA was designed with a rectangular cross-sectional area, termed as "rectangular CA," and was excited with a ceramic material that exhibited a permittivity value of 21. The study of the ReBiT array antenna was designed for a target resonant frequency at 2.30 GHz and to achieve an antenna return loss of less than -10 dB to accommodate high radiation efficiency as well as the miniaturized antenna.

Manuscript received December 28, 2011; revised March 23, 2012; accepted June 25, 2012. Date of publication August 03, 2012; date of current version November 29, 2012.

F. H. Wee and F. Ghani are with the School of Computer and Communication Engineering, Universiti Malaysia Perlis, Perlis, Malaysia (e-mail: weefwenhoon@gmail.com; faridghani@unimap.edu.my).

F. Malek is with the School of Electrical Systems Engineering, Universiti Malaysia Perlis, Perlis, Malaysia (e-mail: mfareq@unimap.edu.my).

A. U. Al-Amani are with the School of Materials and Mineral Resources Engineering (e-mail: srimala@eng.usm.my; ibnuazlan2005@yahoo.com).

Color versions of one or more of the figures in this communication are available online at http://ieeexplore.ieee.org.

Digital Object Identifier 10.1109/TAP.2012.2211557

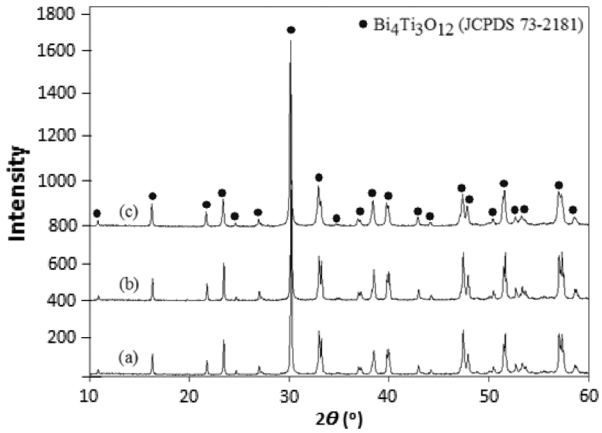

Fig. 1. XRD pattern of the BiT powder at different calcination temperatures for 3 h: (a) 900°C, (b) 1000°C, and (c) 1100°C.

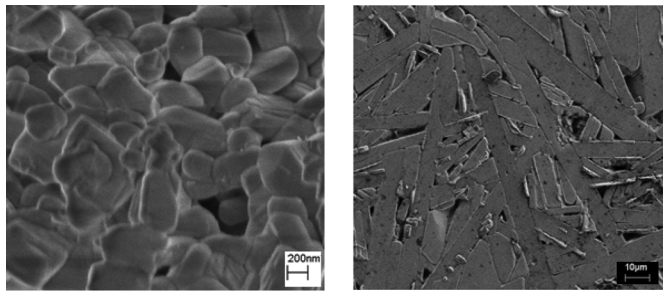

(a) (b)

Fig. 2. FESEM image of BiT: (a) calcined powder at 750°C for 3 h and (b) sintered bulk ceramic at 1100°C for 3 h.

II. Analysis of Bulk Bismuth Titanate (BIT)

A. Sample Preparation

In this study, the raw materials used were bismuth pentahydrate and titanium (IV) isopropoxide. Both raw materials were dissolved separately into a mixture of 2-methaoxyethanol with acetylacetone, forming a Ti solution and a Bi solution. Both solutions were mixed and heated at 80°C to form a sticky gel and combusted to produce combusted powder. The calcination process was conducted at high temperature and pressure, i.e., 750°C and 100 MPa, respectively, to form a green body. Sintering was conducted at 1100°C for densification purposes.

B. Characterization

The X-ray diffraction (XRD) pattern in Fig. 1 shows that the BiT crystalized as the temperature increased from 900°C to 1100°C. The peak in Fig. 1 is centered at 30°, which is the stable phase of pure BiT at the high sintering temperature. This peak shows that the precursor was converted completely into the desired BiT compound. Field Emission Scanning Electron Microscopy (FESEM) micrographs of the BiT powder and the sintered pellet are shown in Fig. 2. It can be seen from the figure that extensive grain growth occurred, which led to platelet formation on the order of 200 nm to 10 μm. The platelets of BiT form a brick wall-like structure by aligning on top of each other, as expected with less platelets damaged during sample preparation.

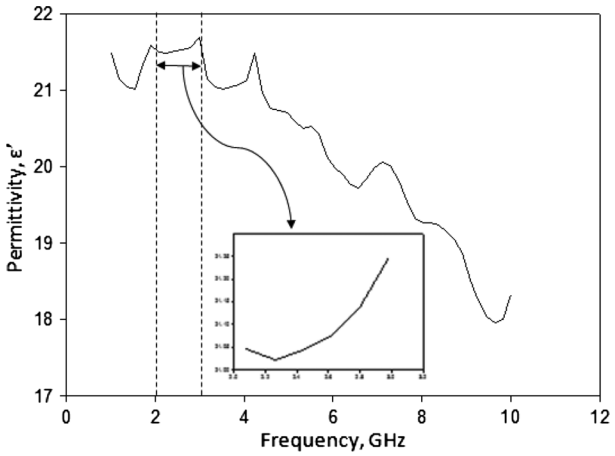

Fig. 3. Permittivity of BiT ceramic at 1 to 10 GHz.

TABLE I
PERMITTIVITY OF BIT AT FREQUENCIES FROM 2 TO 3 GHz

Frequency, GHz	Permittivity, ε	loss tangent, tan δ
2.0800	21.05	0.05
2.2600	21.02	0.06
2.4400	21.05	0.07
2.6200	21.08	0.07
2.8000	21.14	0.07
2.9800	21.25	0.08

We also investigated a new aspect of the development and utilization of the Agilent 85070B High Temperature Dielectric Probe Kit in measuring the permittivity of the BiT ceramic material. The frequency dependence of permittivity for BiT ceramic is shown in Fig. 3. As can be seen, the parameter has a strong dependence on frequency, with the permittivity decreasing as frequency increases; however, for the frequency range of 2 to 3 GHz, the average permittivity and loss tangent are 21 and 0.07 respectively, as shown in Table I. Tests of BiT exhibited low losses, with loss tangent values typically in the order of 0.05 with a tendency toward higher losses up to 0.08 at higher frequencies. The low-loss tangent values were obtained because BiT is free of conducting material, so it has no current flowing on its surface.

Measurement of the radiation pattern was performed in an anechoic chamber, as shown in Fig. 4. The anechoic chamber was used to maximize the effectiveness and efficiency of the measurement space by reducing electromagnetic reflection and improving the quality of the measurements.

The antenna under test (AUT) was rotated through 360 degrees in the theta and phi axes so that E-field and H-field radiation patterns could be measured. The AUT was connected to the transmitting antenna stand in this measurement setup, and the receiving antenna was a circular polarization antenna that allowed the signal from the AUT to be measured from all angles. To measure the gain of antennas, the received power P_{AUT} of the AUT is measured. In this measurement, the receiving antennas must be matched to their loads (the receiver). The calculation of the gain of the AUT in dB uses the Friis transmission equation. The measurement leads to the following system of equations:

$$G_{AUT(\mathrm{dB})} + G_{0(\mathrm{dB})} = 20log_{10}\left(\frac{4\pi R}{\lambda}\right) + 10log_{10}\left(\frac{P_{AUT}}{P_o}\right) \quad (1)$$

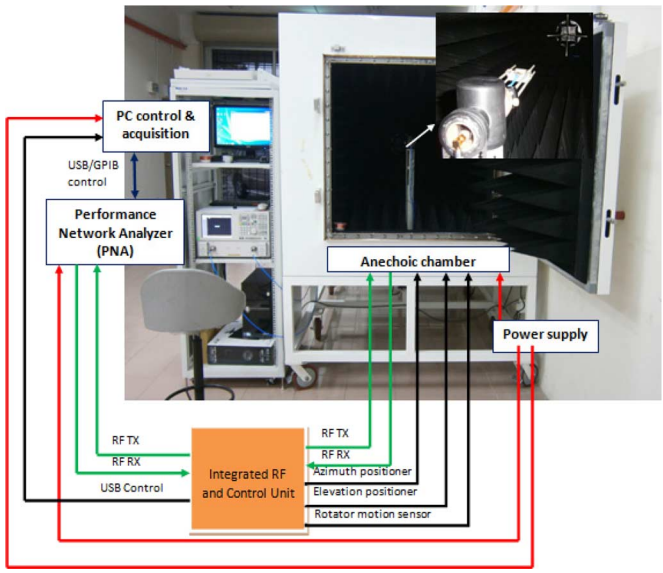

Fig. 4. Measurement of radiation patterns conducted in a microwave anechoic chamber.

$$G_{GS(\mathrm{dB})} + G_{0(\mathrm{dB})} = 20log_{10}\left(\frac{4\pi R}{\lambda}\right) + 10log_{10}\left(\frac{P_{GS}}{P_o}\right) \quad (2)$$

where $G_{AUT(\mathrm{dB})}$ is the gain of the AUT antenna; $G_{GS(\mathrm{dB})}$ is the gain of the gain standard; and $G_{0(\mathrm{dB})}$ is the gain of the transmitting antenna. From (1) and (2), we derived the expression for the gain of the test antenna as follows:

$$G_{AUT(\mathrm{dB})} = G_{GS(\mathrm{dB})} + 10log_{10}\left(\frac{P_{AUT}}{P_{GS}}\right) \quad (3)$$

If the AUT antenna is circularly or elliptically polarized, two orthogonal, linearly-polarized gain standards must be used in order to obtain the partial gains corresponding to each linearly-polarized component. The total gain of the test antenna is

$$G_{AUT(\mathrm{dB})} = 10log_{10}(G_{AUTv} + G_{AUTh}) \quad (4)$$

where G_{AUTv} is the dimensionless gain of the AUT antenna measured with the vertically-polarized gain standard, and $G_{\mathrm{AUT}h}$ is the dimensionless gain of the AUT antenna measured with the horizontally-polarized gain standard.

To record the measurement data and radiation patterns, Passive Measurement software (PMS), integrated with the anechoic chamber, was used. Measurement data were collected at specific points in order to determine the radiation pattern. The PNA calculated the antenna gain, directivity and efficiency as well as conducting 2-D and 3-D test. The test results for each angle and the displayed radiation pattern were plotted.

III. ANTENNA CONFIGURATION AND DESIGN

The most popular technique for reducing the size of a printed antenna is the use of a high-dielectric material for the radiating part. In doing so, the guided wavelength underneath the patch can be reduced and hence the size of the resonating patch also can be reduced. The reduction ratio is approximately related to square root of ε'. Existing patch antenna using an ε' values in the range of 1 to 20 have a dimension of about 0.44λ [3]. However, for the BiT antenna using an ε' value of 21, the

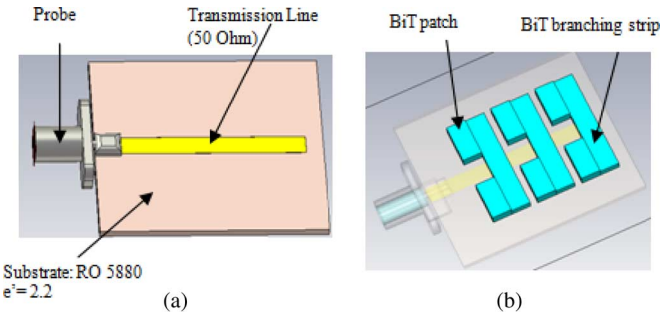

Fig. 5. Configuration of the multi-layers and their optimized dimensions, (a) first layer, (b) second layer.

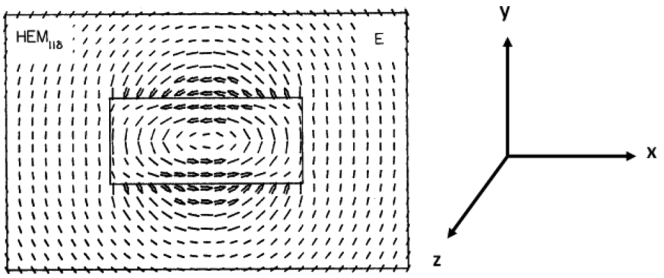

Fig. 6. Electric field of ceramic at HEM_{11}.

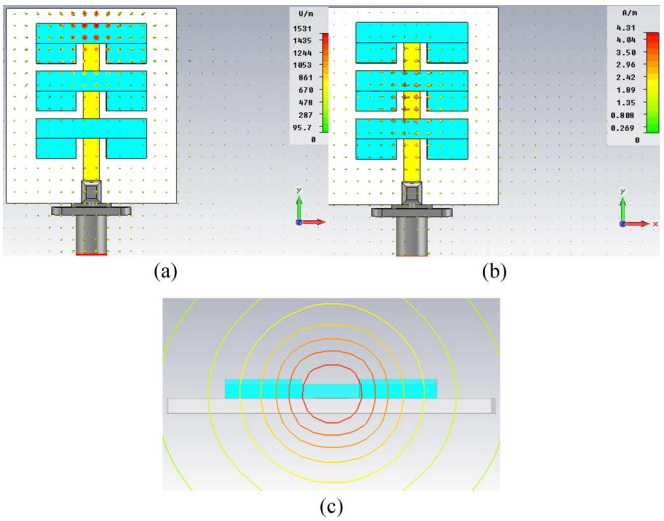

Fig. 7. (a) Electric field pattern (left) and magnetic field pattern (right) of HEM_{11}. (b) Field propagation behavior when a port is placed parallel to the strongest field.

size of the patch is reduced to about 0.20λ. To further reduce the size, array elements of BiT materials were introduced. Depending on the number of BiT elements added to the patch antenna, a size reduction of about 28% can be achieved. As an actual demonstration, a recently developed proposed antenna using an ε' value of 21 and two-, four- and six-elements of BiT achieved a patch of $25 \times 22 \times 1.6$ mm at a frequency of 2.30 GHz (Fig. 9). Because the antenna is small structure from an electrical perspective, the antenna provided nearly complete spherical coverage as shown in the measured patterns in Fig. 10.

The proposed antennas have two layers, which are shown in Fig. 5. The first layer is a transmission line, which is shown in Fig. 5(a). Its optimal dimensions are presented in Fig. 7. The transmission line uses

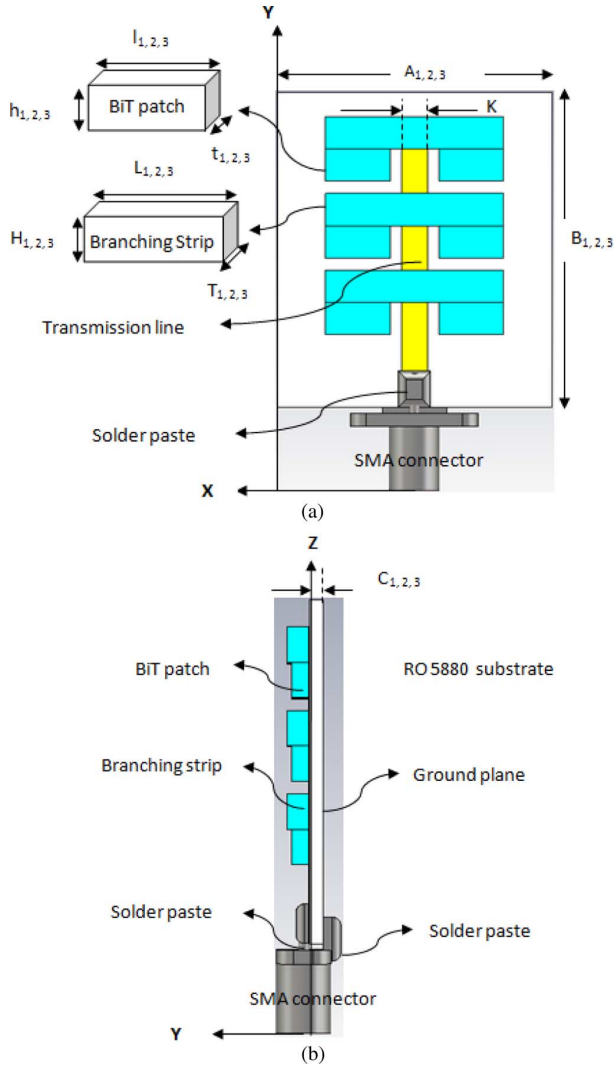

Fig. 8. Geometry layout of proposed ReBiT array antenna (a) front view (b) side view.

copper, which is a conducting material, in order to function as a feeding channel.

For the second layer of this investigation, the effectiveness of BiT was determined as power division and radiating element. The novelty of this design is the BiT ceramics that have high permittivity. The proper sizes, positions, and shapes were added to the second layer of the antenna, as shown in Fig. 5(b). The typical mode of operation in shielded environment is TE_{01}, while in an open space, the typical mode is HEM_{11} which the ceramic material acts as a radiator. Fig. 6 shows the electric field of the ceramic material in the HEM_{11} mode.

The electric field is strong at the top and bottom surfaces of the ceramic, and this field propagation behavior indicates that a port can be placed parallel to the strongest field, i.e., along the y-axis of the resonator, in order to couple to this mode effectively. This technique was utilized in the design of the ReBiT. In order to excite the HEM_{11} mode, a port can be inserted close to the perimeter of the resonator, as shown in Fig. 7.

Three types of ReBiT array antenna were designed in this communication. There are two-, four-, and six-elements of ReBiT in the array antenna, each of which has different dimensions. The geometry of the proposed ReBiT array antenna is shown in Fig. 8, indicating both the front view and the side view. The antenna was designed on a low-loss,

TABLE II
REBIT SIZE FOR TWO, FOUR, AND SIX ELEMENTS OF BIT

Number of elements / Dimension of elements	2 BiT elements	4 BiT elements	6 BiT elements
Antenna (A_n x B_n x C_n) mm	$A_1 = 30$	$A_2 = 27$	$A_3 = 22$
	$B_1 = 33$	$B_2 = 29$	$B_3 = 25$
	$C_1 = 1.6$	$C_2 = 1.6$	$C_3 = 1.6$
Branching Strip (H_n x L_n x T_n) mm	$H_1 = 2.5$	$H_2 = 2.5$	$H_3 = 2.5$
	$L_1 = 27$	$L_2 = 25$	$L_3 = 20$
	$T_1 = 1$	$T_2 = 1$	$T_3 = 1$
Patch (h_n x l_n x t_n) mm	$h_1 = 2.5$	$h_2 = 2.5$	$h_3 = 2.5$
	$l_1 = 4.5$	$l_2 = 3.5$	$l_3 = 3$
	$t_1 = 0.8$	$t_2 = 0.8$	$t_3 = 0.8$

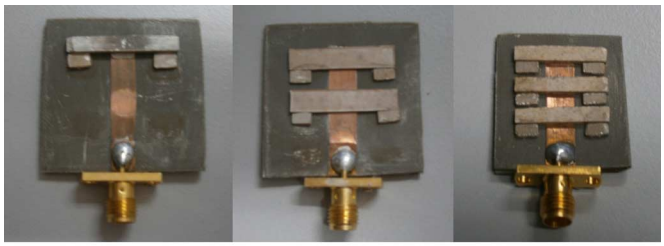

(a) (b) (c)

Fig. 9. Photograph of fabricated ReBiT array antennas (a) two-, (b) four-, and (c) six-BiT ceramic elements.

RT/Duroid 5880, commercial microwave substrate from Rogers Corporation (www.rogerscorp.com) with a permittivity of 2.20, where the BiT branching strips and patches exhibit permittivity of 21. The width of the transmission line was optimized at $\mathrm{K} = 4.6\ \mathrm{mm}$ in order to achieve input impedance matching of 50 Ω.

There are typically more losses associated with corporate feeds than series feeds due to radiation from the discontinuities and the longer lengths of the lines. Hence, this novel series linear array of ReBiT elements has the potential to reduce the high loss effect by utilizing non-conducting material that made of ceramic. This is due to the use of conventional conducting material will caused high loss thus, affect the antenna radiation performance.

From Table II, the size of the six-BiT element antenna can be observed as the smallest compared to both two- and four-BiT elements of ReBiT array antennas. In this case, the number of elements and the wavelength of the ceramic array antenna, λ_g, can be approximated using:

$$\lambda_g = \frac{\lambda_0}{\sqrt{n\varepsilon_r}} \tag{5}$$

where λ_g is the guided wavelength in CA, λ_0 is the free-space wavelength, ε_r is the dielectric constant of the ceramic, and n denotes the number of ceramic elements. Thus, a small size of ceramic is obtained with high-number of ceramic elements. This condition happens due to the present of the large area electromagnetic wave in the ceramic.

In addition to the modeling design, prototypes of the ReBiT array antennas with the optimized parameters were fabricated and measured, as shown in Fig. 9. This was done in order to ensure good agreement among their performances.

IV. RESULTS AND DISCUSSION

Fig. 9 shows a graph of the return loss of the six elements of the ReBiT array antenna converted into log magnitude in dB.

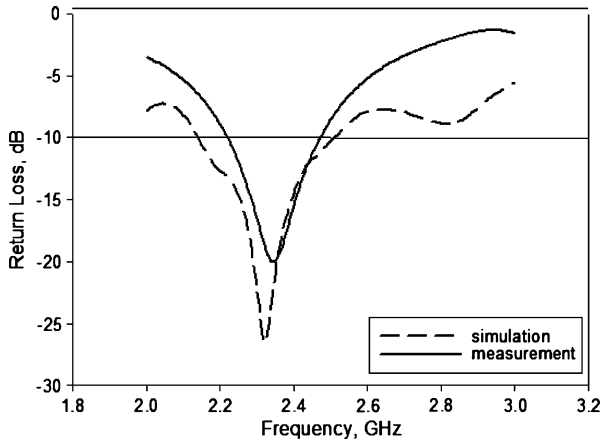

Fig. 10. Simulated and measured return losses of the ReBiT array antennas.

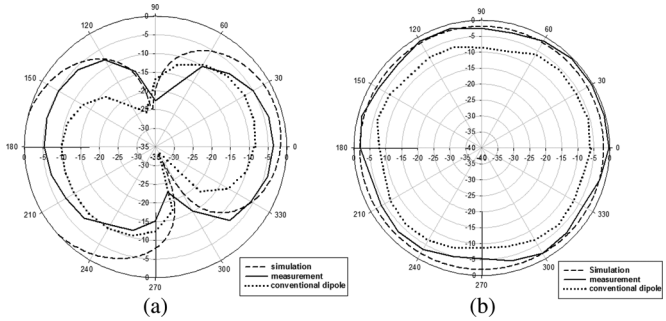

(a) (b)

Fig. 11. 2-D radiation pattern (a) E-plane (b) H-plane.

The simulation and measurement results show that the lowest return loss is -27 dB with an operating bandwidth of 350 MHz. Overall, good agreement was found between the simulated and measured results, although there was a slight discrepancy between them that is believed to be due to the environmental effect and mechanical tolerance, which were neglected in our simulations. The gains and radiation efficiencies of the two-, four-, and six-BiT element ReBiT array antennas at 2.3 GHz are summarized in Table III.

The gain of the two-BiT element was 6.56 dB. This value increased up to a maximum of 7.51 dB for a six-BiT element, which was 1 dB higher than that of the two-BiT element. The reason for such a small change in the gain was that the surface area of the BiT was very small. Hence, interaction between the antenna and the BiT ceramic was minimized. However, the conventional dipole antenna also was simulated and its gain and directivity were measured for comparison with the BiT-array antenna. The conventional antenna achieved about 3.48 dBi and 4.83 dBi in gain and directivity respectively with 71.9% radiation efficiency as compared to 95% for BiT array antenna.

The simulated and measured radiation patterns in 2-D and 3-D views are shown in Figs. 11, 12, and 13 respectively. Both the E-field and H-field patterns incurred a slight change in shaped which in addition to errors in the manufacturing process were due to the imprecision of the dimensions of the BiT elements. The radiation pattern of the conventional dipole antenna exhibited omni-directional as BiT array antennas. For both BiT and conventional dipole antenna in Fig. 12 and 13 respectively, there were no top and bottom lobes at the rear end of the radiation pattern while the main directivity was directed at the vertical plane, which formed an omni-directional signal level in the H-plane.

BiT array antennas achieve about 15% of aperture efficiencies that vary from 12% to 20% with 7 dB gain. Since the BiT has zero conduction loss, there is no longer any power dissipation from the ceramic.

TABLE III
GAIN, DIRECTIVITY, AND RADIATION EFFICIENCY OF REBIT ARRAY ANTENNAS

Parameter (2.3 GHz)	Number of BiT elements (simulation)			Number of BiT elements (measurement)			Conventional dipole
	2	4	6	2	4	6	
Gain (dBi)	6.56	7.19	7.51	6.11	6.42	7.21	3.48
Directivity (dBi)	7.17	7.70	7.91	7.09	7.24	7.75	4.83
Radiation Efficiency (%)	91.4	93.4	95.0	86.2	88.5	93.0	71.9

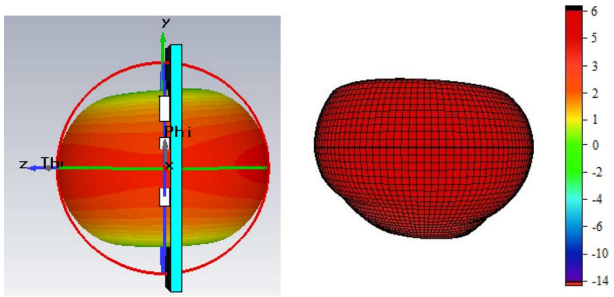

(a) (b)

Fig. 12. Radiation pattern of ReBiT in 3-D view (a) simulated (b) measured.

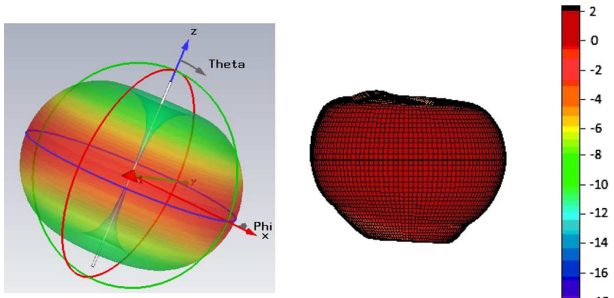

(a) (b)

Fig. 13. Radiation pattern of conventional dipole antenna in 3-D view (a) simulated (b) measured.

However, there is conduction loss occur only in the transmission line. Thus, the power output of the antenna is almost the same as the power input. The efficiency of the aperture is defined as:

$$n = \frac{A_{eff}}{A_p} \tag{6}$$

where η is the aperture efficiency, $A_{\rm p}$ is the physical size of the aperture, and $A_{\rm eff}$ is the effective aperture. The maximum equivalent area of an arbitrary antenna is related to its gain by:

$$A_{eff} = \frac{\lambda^2}{4\pi} G \tag{7}$$

where $A_{\rm p}$ is the physical area of the BiT array antenna.

V. CONCLUSIONS

In this communication, the application of BiT in an array antenna was conducted successfully. The antenna exhibited acceptable bandwidths, reflectivity, and radiation characteristics for WiMAX applications, as well as low production cost due to its unique ceramic fabrication process. In future work, the use of BiT for other types of antennas should be investigated in order to determine the improvement in performance that can be achieved in terms of bandwidth in particular and optimization of the radiation pattern in general.

REFERENCES

[1] M. F. Ain, Y. M. Qasaymeh, Z. A. Ahmad, M. A. Zakariya, M. A. Othman, A. A. Sulaiman, A. Othman, S. D. Hutagalung, and M. Z. Abdullah, "A novel 5.8-GHz array dielectric resonator antenna," *Progr. Electromagn. Res. C*, vol. 15, pp. 201–210, 2010.

[2] M. F. Ain, S. I. S. Hassan, J. S. Mandeep, M. B. Othman, B. M. Nawang, S. Sreekantan, S. Hutagalung, and Z. A. Ahmad, "2.5-GHz dielectric resonator antenna," *Progr. Electromagn. Res.*, vol. PIER 76, pp. 201–210, 2007.

[3] R. K. Gangwar, S. P. Singh, and D. Kumar, "A modified fractal rectangular curve dielectric resonator antenna for WiMAX application," *Progr. Electromagn. Res. C*, vol. 12, pp. 37–51, 2010.

[4] R. V. Petrov, A. S. Tatarenko, S. Pandey, G. Srinivasan, J. V. Mantese, and R. Azadegan, "Miniature antenna based on magnetoelectric composites," *Electron. Lett.*, vol. 44, no. 8, Apr. 10, 2008.

[5] J. Li, "An omnidirectional microstrip antenna for WiMAX applications," *IEEE Antennas Wireless Propag. Lett.*, vol. 10, 2011.

[6] S. Prabhu, J. S. Mandeep, and S. Jovanovic, "Microstrip bandpass filter at S-band using capacitive coupled resonator," *Progr. Electromagn. Res.*, vol. PIER 76, pp. 223–228, 2007.

[7] R. K. Mongia, A. Ittipiboon, and M. Cuhaci, "Measurement of radiation efficiency of dielectric resonator antennas," *IEEE Microw. Guided Wave Lett.*, vol. 4, pp. 80–82, Mar. 1994.

[8] A. A. Kishk, X. Zhang, A. W. Glisson, and D. Kajfez, "Numerical analysis of stacked dielectric resonator antenna excited by a coaxial probe for wideband applications," *IEEE Trans. Antennas Propag.*, vol. 51, pp. 1996–2006, Aug. 2003.

[9] A. A. Kishk, "Wide-band truncated tetrahedron dielectric resonator antenna excited by coaxial probe," *IEEE Trans. Antennas Propag.*, vol. 51, pp. 2913–2917, Oct. 2003.

[10] M. T. Lee, K. M. Luk, K. W. Leung, and M. K. Leung, "Small dielectric resonator antenna," *IEEE Trans. Antennas Propag.*, vol. 50, pp. 1485–1487, Oct. 2002.

[11] S. Sreekantan, A. F. M. Noor, Z. A. Ahmad, R. Othman, and A. West, "Structural and electrical characteristics of crystalline barium titanate synthesized by low temperature aqueous method," *J. Mater. Process. Technol.*, vol. 195, no. 1–3, pp. 171–177, 2008.

[12] J. Clerk Maxwell, *A Treatise on Electricity and Magnetism*, 3rd ed. Oxford: Clarendon, 1892, vol. 2, pp. 68–73.